



Maximization of Sum Throughput in LTE Heterogeneous Network using Region Splitting-Based Resource Partitioning Scheme

S. Ezhilarasi¹ · P. T. V. Bhuvaneshwari¹

Accepted: 14 June 2021 / Published online: 28 June 2021

© The Author(s), under exclusive licence to Springer Science+Business Media, LLC, part of Springer Nature 2021

Abstract

LTE Advanced (LTE-A) technology has been developed by the third generation partnership project in order to facilitate increase in mobile data traffic. In LTE-A network, an efficient resource partitioning scheme is needed to increase the system throughput through the mitigation of Inter Cell Interference (ICI). The objective of this research is to enhance the sum throughput of macrocell through an proposed Region splitting based Resource Partitioning scheme (RRP). In this scheme, the macrocell is partitioned into three regions, namely inner, centre and outer. In a cluster of three cells, the available frequency spectrum is divided into four non-overlapping parts, out of which three parts of the spectrum are shared by outer and inner region. The remaining part is shared by the centre region. However, the overlaid femtocells partially shares the spectrum of macrocell. The performance of the proposed RRP scheme in terms of sum throughput, sub channel utilization and Jain's Fairness index is analysed for both heuristic and optimal region radii approaches. The region radii that result in maximum and optimal sum throughput are analyzed by the proposed RRP scheme. Using Monte Carlo simulations, the radii of both inner and centre region are varied and the region radii that result in optimum sum throughput are configured as the optimal radius. The proposed scheme is compared with the traditional Soft Frequency Reuse scheme with respect to performance metrics. From the result, it is inferred that the sum throughput of macrocell achieves a maximum enhancement of 167.62 and 108.42 % by the proposed scheme of heuristic and optimal region radii approaches respectively.

Keywords Inter Cell Interference · Long Term Evolution -Advanced · Region Splitting based Resource Partitioning · Region radius · Soft Frequency Reuse

Abbreviations

eNB evolved node B
eICIC enhanced inter-cell interference coordination

✉ S. Ezhilarasi
ezhilvish@yahoo.co.in

P. T. V. Bhuvaneshwari
ptvbmit@annauniv.edu

¹ Department of Electronics Engineering, Madras Institute of Technology, Anna University, Chennai, India

FFR	Fractional frequency reuse
FRF	Frequency reuse factor
FBS	Femto base station
HetNet	Heterogeneous network
ICI	Inter-cell interference
LTE	Long term evolution
LTE-A	Long term evolution advanced
MBS	Macro base station
MUE	Macro user equipment
OFDMA	Orthogonal frequency division multiple access
QoS	Quality of service
RRP	Region splitting based resource partitioning
SINR	Signal-to-interference -plus-noise ratio
SFR	Soft frequency reuse
3GPP	Third generation partnership project

List of symbols

Ω_{MU}	Sum throughput of macrocell.
M	Macrocell.
F	Femtocell.
m	Set of macrocells.
L	Set of femtocells.
K	Total number of macrocells.
χ_U	Set of MUEs per cell.
MU	Total number of MUEs per macrocell.
I_z	Inner region.
C_z	Centre region.
O_z	Outer region.
B	Total amount of spectrum.
$\beta_{\chi,a}$	Sub-band allocation index.
Φ	Total number of sub channels.
Φ_{min}	Minimum of one sub channel assigned to each region.
Φ_I	Amount of sub channels assigned to inner region users.
c	Amount of sub channels to centre region users.
Φ_O	Amount of sub channels to outer region users.
χ_{MI}	Radius of inner region.
χ_{MC}	Radius of centre region.
χ_{MO}	Radius of macrocell.
χ_F	Radius of femtocell.
R_I	Ratio of χ_{MI} and χ_{MC} .
R_C	Ratio of χ_{MC} and χ_{MO} .
χ_{do}	Minimum distance between MUE and eNB.
η_{IMU}	SINR experienced by inner region users.
η_{CMU}	SINR experienced by centre region users.
η_{OMU}	SINR experienced by outer region users.
ψ_{MU}	Data rate achieved by MUE.
JI_{MU}	Jains Fairness Index.

1 Introduction

In the current cellular network scenario, the mobile data traffic is drastically increasing due to the proliferation of mobile activities, namely social media usage, voice or video calls, mobile chat, and mobile e-commerce etc. [1]. The next generation cellular network aims at providing a solution to meet out the above requirements. Some of the key techniques recommended for the improvement of system capacity are (i) advancements in network architecture (ii) deployment of Heterogeneous Network (HetNet) (iii) convergence of information and communication technology.

The Orthogonal Frequency Division Multiple Access (OFDMA) is a multiple access technique which is used for downlink transmission in Long term evolution (LTE), LTE-Advanced (LTE-A) and Fifth Generation (5G) networks [2]. Third Generation Partnership Project (3GPP) has introduced LTE in release 8 [3] to meet the objective of high data rate, enhancement in system capacity and coverage, scalable bandwidth and low latency. The techniques namely Orthogonal Frequency Division Multiplexing (OFDM), Multiple-Input Multiple-Output (MIMO) and Coordinated Multi Point communication (CoMP) etc. are introduced for achieving the above objectives [4]. In release 9 of 3GPP, HetNet concept has been introduced to enhance the coverage and capacity of LTE indoor users [5]. However, this imposes various challenges, namely, inter-cell and intra-cell cross-tier interference, load balancing, handover, and scheduling [6]. Further, 3GPP has incorporated additional features namely enhanced MIMO, Carrier Aggregation (CA) and Relay nodes in release 10 to enhance Quality of Service (QoS) of cell edge users [7]. This is referred as LTE-A. However these features enforce several challenges, namely, mobility management, self-organization, back haul signalling and scheduling. The next generation access technology has been introduced in release 14 of 3GPP. It is referred as 5G networks [8]. The objectives of this release are (i) Peak data rate: 20Gbps-DL and 10Gbps-UL (ii) Peak spectral efficiency: 30 bps/Hz-DL and 15 bps/Hz-UL (iii) User plane latency: 0.5 ms-DL and 0.5 ms-UL (iv) Connection density: 1 million devices per sq/km. In order to accomplish the above objective, an enhanced radio access technology known as New Radio (NR) is introduced in release 15 [9]. The various supporting components added in this technology are (i) extension to higher frequency bands (ii) wireless access/backhaul integration (iii) machine-to-machine communication and (iv) flexible duplex. To accomplish the above objectives, the 5G network will be able to support/operate in both LTE band and NR band [10].

In LTE/LTE-A/5G-NR, OFDMA utilizes subcarrier of 15 kHz. The subcarriers are grouped into sub channels. Each sub channel consists of 12 subcarriers of 180 kHz bandwidth. The User Equipment's (UE) can occupy different subcarriers at different instances of time by the adoption of flexible resource partitioning with reuse mechanisms. This can enhance spectral efficiency and multi user diversity gain. Further, it can also reduce Inter symbol Interference (ISI) and Intracell interference [11]. The inter-cell interference (ICI) can be caused whenever the neighboring cells are operating on the same frequency band. This is due to the adoption of frequency reuse mechanism. In such interference limited systems, the cell edge users are severely susceptible to this kind of interference. The factors influencing ICI are high path loss and strong multiple ICI received from the adjacent cells. They can further affect the capacity of the system.

Findings from the literature indicate that, ICI can be considered as one of the major limiting factors that can influence the system performance of LTE/LTE-A/5G-NR [12]. The various solutions are addressed in [13] for improving the throughput of cell edge users

and enhancing the system performance. The ICI mitigation technique for OFDMA based cellular networks is discussed in [14]. It can be classified into three approaches, namely Interference randomization (IR), Interference cancellation (IC), and Interference avoidance (IA). These techniques are implemented either before transmission or after the reception of the signal.

In the first approach, the evolved Node B (eNB) generates randomized interfering signal to suppress the interference experienced by the UEs connected to it. The techniques followed for randomization are cell specific scrambling, interleaving and frequency hopping. The second approach cancels the interference signal at the receiver with the aid of the channel state information estimation mechanism. This results in reduction in latency and complexity. Hence this approach is highly suitable for Uplink (UL) ICI mitigation. In the third approach, static frequency reuse planning schemes are employed for improving the Signal-to-interference-plus-noise ratio (SINR). The transmission power of an eNB is operated within the maximum acceptable limit. In addition, adaptive beam forming is one of the solutions for ICI mitigation where the radiation pattern of the antenna can be changed dynamically with respect to interference level.

Among the above approaches, IA techniques improve the QoS of cell edge users without sacrificing the cell centre throughput. The research focus is restricted to IA based static frequency reuse planning in LTE HetNet to maximize the sum throughput of macrocell. It investigates the influence of region radius and sub channel allocation. A Region splitting based Resource Partitioning (RRP) scheme by heuristic and optimal region radii approach is proposed for achieving the above objective.

The rest of the paper is organized as follows: Section II presents the state-of-the-art approach related to the proposed research. Section III presents the system model of the proposed scheme. Section IV presents the outcome of the proposed scheme with simulation results. Finally, Section V concludes highlighting the contribution of the work and offers suggestions for future work.

2 Literature Survey

In this section various solutions that are provided for mitigating ICI in co channel deployment of femtocell are discussed. This research is limited to frequency partitioning based ICI mitigation techniques. The macrocells are assumed to possess centre excited omni directional antenna.

In [15], the authors have developed frequency reuse scheme with three regions in cooperative relaying for multi-cell OFDMA Systems. In this scheme, the macrocell is divided into centre, middle and edge regions. The total bandwidth is divided into three parts corresponding to three regions. The different combination of Frequency Reuse Factor (FRF) is applied to these regions in order to reduce Co-Channel Interference (CCI). The combinations are $\{1, 3, 7/3\}$, $\{1, 4, 7/4\}$ and $\{1, 3, 6\}$. The inference drawn from the simulation result is outage probability, cumulative distribution function and average spectral efficiency of the developed scheme performs better than non cooperative scheme.

In [16], the authors have presented the optimal Fractional Frequency Reuse (FFR) scheme with dynamic resource allocation strategy. The total throughput and User Satisfaction (US) metrics are calculated as performance metrics. The region radius which results in a maximum value of US for both static and moving users is taken as optimal and maximum US as reflecting a uniform distribution of resource among the users. This research work

is compared with Integer frequency reuse 1 (IFR1) and Integer frequency reuse 3 (IFR3) schemes. The inference from the simulation results is that, this work outperforms the existing ones in terms of total throughput.

In [17], the authors have developed the Optimal Static FFR (OSFFR) scheme. The macrocell coverage is partitioned into the centre and the edge zone with six sectors. The total spectrum is divided into seven sub-bands. Among the seven, only one sub-band is used by the centre zone MUEs with FR1. The remaining six sub-bands are utilized by the edge zone MUEs with FR6. Further, the femtocell partially shares the sub-band of the macrocell for carrying out a reduction in inter and intra-cell cross-tier interferences. The complexity increases due to the division of more sub-bands and sectors. The metrics, namely outage probability, network throughput, and spectral efficiency are considered for the purpose of comparison. The conclusion from the result is that the developed scheme outperforms the existing ones, namely, strict FFR, soft FFR, and FFR-3. However, it is found that a large number of sub-bands are utilized by the femtocells can be seen.

In [18], the authors have analyzed the (i) interference between the macrocell and the femtocell and (ii) between femtocells using the power control technique. They have suggested water filling and Adaptive spectral mask algorithms (ASMA). In ASMA, the MUE makes a periodic update of its total interference power experience on each sub-carrier with respect to the interference causing FBS to MBS. MBS applies spectral masks over FBS through the periodic updates. The convergence of the presented algorithm is computed with respect to three factors, namely, feedback signals determined by MUE, the transmission time of feedback, and FBS transmission power. The performance loss and the percentage of interfering MUEs have been analyzed. Additional overhead due to the feedback signal is identified as the limitation of the developed method.

In [19], the authors have analyzed LTE and LTE-A multi-cell system performance through simulation framework. In this framework, the macrocell is divided into inner and outer regions. The total frequency resources are divided into four sub-bands, namely A, B, C, & D. Sub-band 'A' is used by the MUEs present in the inner region in both the environments. The outer region MUE utilizes the remaining three sub-bands. A partial amount of resources is shared by the femtocells for the purpose of mitigation of ICI. The optimal region radius has been determined by three metrics, namely total throughput, Jain's Fairness Index (JI), and weighted throughput. The optimality of FFR scheme has been obtained by varying the inner region radii and resource blocks. The inference from the simulation results is that the weighted throughput approach outperforms the other two approaches.

The authors of [20] have analysed the cross-tier interference between the macrocell and the femtocell using frequency partitioning methods. In this method, the coverage of macrocell is divided into inner and outer regions which are sectored by three directional antennas. The entire frequency band is allocated exclusively for uplink and downlink transmission. It is divided into four non-overlapping parts. One part of the band is assigned to the inner region MUE / FUE. The remaining three parts are shared by both macrocell and femtocell. The outcome of the simulation study is compared with the theoretical results in terms of average per-channel downlink and uplink rates of macrocell and femtocell. The results lead to that the interference power having a smaller impact on inner-region radii. The limitation observed is that the impact of different radius of the inner region has not been analysed.

In [21], the authors have presented unified frequency reuse (UFR) framework for the next generation HetNets. In this frame work, the different tier networks utilizes 54%, 18%, 20% and 8% of total spectrum which is represented as b1, b2, b3, & b4 frequency bands respectively. The frequency bands b1 & b2 are utilized by macrocell with FRF-3 and micro-cell respectively. Similarly, b3 & b4 are utilized by small cell with FRF-2 and random

distribution of coverage points respectively. The authors analyzed the network performance in terms of spectral efficiency, area throughput and energy efficiency which outperforms than the classical Frequency Reuse (FR) and FFR schemes.

In [22], the authors presented FRF for irregular geometry based heterogeneous cellular networks. The macrocell is divided into centre and edge region with three sectors which is referred as sectorized FFR scheme. The MBSs and FBSs are randomly deployed by statistical modeling of Hard Core Point Process (HCPP) and Poisson Point Process (PPP). In this scheme, the cell partitioning is done through the two parameters namely SINR threshold of MUE and FUE. The total spectrum is divided into four sub-bands where three sub-bands are utilized by edge region of macrocell which is reused by the centre region of femtocell. Similarly, the remaining is used by centre region of macrocell and edge region of femtocell in order to mitigate cross-tier interference. The dynamic spectrum allocation strategy is followed with respect to area of coverage. From the simulation results, the aggregate throughput and cumulative distribution function of MUEs and FUEs results with better performance than strict-FFR and FFR-3 schemes.

In [23], the authors have presented the resource partitioning scheme in order to mitigate the interference between macro and femtocells. The macrocell coverage area is partitioned into three layers, namely, centre, intermediate, and outer along with six sectors. 18 sub areas have been considered in all. The total bandwidth is divided into seven sub-bands, namely A, B, C, D, E, F, and G. In the developed scheme, the MUE closer to eNB and FUE away from eNB share the higher sub-bands in order to improve the total throughput and spectral efficiency. This approach limits the interference in co-channel, cross-tier and co-tier between macro and femtocell. Throughput of macrocell, femtocell, and total throughput for varied number of femtocells are computed through simulation. The scheme presented is superior to the existing schemes, namely, FFR-3, 3-layer/3-sector FFR, and OSFFR. In particular, the OSFFR scheme exhibits better throughput of femtocell due to lesser co-tier interference.

In [24], the authors have analyzed the throughput and the capacity of the LTE network using the Soft Partial Frequency Reuse (SPFR) method, wherein the macrocell is divided into Central Area of Cell (CAC) and Boundary Area of Cell (BAC). The CAC area is further partitioned into CAC_{far} and CAC_{near} . The total spectrum is assigned as 50% and 10% to CAC and BAC respectively. Further, 20% of soft band is utilized by CAC_{near} and BAC with respect to network traffic. The remaining unused 20% is reserved for future use. The inference from the simulation result is that the network throughput and cell capacity are enhanced as a result of provisioning of 20% of the soft band when compared with the FFR scheme.

The authors of [25] presented an adaptive self-organizing frequency reuse approach for deriving the optimal value of inner radius. The coverage of each macrocell is divided into two regions, namely, inner and outer. The available frequency resource is divided into four sub-bands. In this approach, MUE of inner region is allowed to use any of the sub-bands to ensure the total interference received by all MUEs in the inner region being kept minimal. The authors have used the simulation result for the determination of the optimal value of the inner radius by considering the closeness between the total throughput of outer and inner regions. The optimality is investigated with respect to the total transmission power of eNB, cell radius and total cell throughput. The investigation shows that the presented work outperforming the traditional FFR scheme.

In [26], the authors presented multi-layer soft frequency reuse scheme for 5G heterogeneous cellular networks. In this scheme, the macrocell is divided into four circular zones with different power allocation in which first and fourth layer forms one SFR while second

and third forms another SFR scheme. The spectrum allocated for small cell increases with the increase of layers. The authors have analyzed network throughput, spectral efficiency and outage probability metrics for different layers such as 2, 4 & 8. The inference drawn is that the performance metrics of layer 8 outperforms than 2 & 4.

In [27], the authors have presented joint spectral efficiency and energy efficiency in FFR based wireless HetNets. In this work, Area Spectral Efficiency (ASE) and Area Energy Efficiency (AEE) are jointly analyzed with respect to range expansion, FFR and proportional fairness allocation strategy. A theoretical framework is derived based on these metrics. The outcome of joint performance is referred as Area Spectral Energy Efficiency (ASEE) which is optimized in terms of power reduction factor and bandwidth partition factor. The performance of ASE, AEE and ASEE are analyzed under two scenarios namely equal bandwidth and data rate to each UE. It is observed that, ASEE has balanced the performance of both ASE and also theoretical results are validated with simulation outcome in terms of average user spectral efficiency.

In [28], the authors have presented the novel FFR scheme with efficient resource allocation mechanism to mitigate CCI in LTE-A HetNets. The whole macrocell coverage area is partitioned into three layers, namely, center, middle, and outer and each layer is further divided into three sectors. Therefore in total of 9 zones can be considered. The total bandwidth is divided into seven sub-bands, namely A, B, C, D, E, F, and G. The sub-band G is only reserved for center layer MUEs, whereas the remaining sub bands are utilized by each sector of middle and outer layer MUEs. However, the femtocells were reuse the sub-band of middle and outer layer of macrocell on the basis of detected value of RSRP. Throughput and efficiency of the system are computed through simulation, and found to be better than the existing schemes namely OSFFR, FFR-3, and FFR-3R. One of the limitations is identified as less spectral efficient in the developed method due to the reserved sub-band assigned in the center layer of macrocell.

The works presented in the above literature, clearly mention the factors to be considered in the resource partitioning scheme that can be made between macro and femtocells. They are (i) division of macrocell region, (ii) region radius, (iii) static frequency reuse and (iv) deployment nature of FBS, its transmission power and position. The authors in [16, 19], & [25] have concluded that the region radius which maximizes user satisfaction, total throughput, weighted throughput, JI, and throughput of regions is considered as the optimal radius. The impact of other factors namely, density of users and area of region radius has not been considered in the optimization process.

The work presented in [24] is limited to macrocell environment. The works in [17, 20], & [23] operate macrocell in both omni directional and directional antennas. Allocation of more sub-bands to femtocell, causes a smaller outage probability of the macrocell. In [20], the analysis is restricted to two different inner region radii. In [18], the macrocell applies spectral masks over the femtocell for reducing the interference. This leads to a reduction in spectral efficiency. Further, an increase in overhead is witnessed due to the feedback signal. In [21], due to stochastic deployment of users in the small cells, static planning of sub-band strategy adopted in these small cells leads to reduction in spectral efficiency. In [26], due to increase in the layers of macrocell, complexity involved in the determination of optimal region radii increases.

In [15], the analysis is restricted to homogeneous environment and increasing the complexity by the adoption of different reuse scheme in the macrocell of three regions. Further it is observed that, CCI is minimal at the edge region than the other two regions. In [26], the cross-tier interference is very significant when MUE is placed in the transition region and the impact of femtocells on the performance analysis is not considered. In [27], the

performance analysis is restricted to two scenarios namely equal bandwidth and data rate. Here the impact of dynamic resource allocation strategy with optimization is not considered. In [28], the following limitations were found: They are intra cell handover problems due to directional antennas and higher priority to center layer MUEs by the assignment of dedicated sub band.

In the proposed research, Region splitting based resource partitioning (RRP) scheme with efficient resource allocation strategy is developed for overcoming the above limitations. The objective of the proposed research is to enhance the sum throughput of the macrocell.

In the proposed scheme, the entire macrocell region is divided into three regions, namely, inner, centre, and outer. The femtocell deployed in each region partially shares the frequency resources of macrocell. An additional third region is included for mitigating ICI, inter and intra-cell cross-tier interference. The entire frequency band is partitioned into four non-overlapping sub-bands in a cluster of 3 cells. The sub-bands are 'a', 'b', 'c' & 'd'. The first three sub-bands 'a', 'b' & 'c' are utilized by the outer region MUEs. The remaining sub-band 'd' is further divided into three non overlapping parts, namely 'd₁', 'd₂', & 'd₃'. It is utilized by the centre region. In addition, the inner region of macrocell partially shares the sub-band of the outer region of the neighboring cells. Similarly, the femtocells present in the inner region makes partial share the sub-band of the outer region of the same cell. This leads to the elimination of intra-cell cross-tier interference.

In case of the centre region, the femtocell makes partial share of the sub-band of the inner region of the macrocell. This may cause intra-cell cross-tier interference when MUE is placed within the vicinity of FBS. Similarly, the femtocell deployed in the outer region shares the sub-band of the centre region of the neighbouring macrocell. This kind of resource partitioning eliminates the intra-cell and the inter-cell cross-tier interferences thereby increasing the system throughput. Hence, three region approach are employed in the proposed RRP scheme for enhancing the sum throughput of the macrocell. In the proposed scheme, the impact of sum throughput on region radii and its corresponding sub channel allocation by heuristic and optimal region radii approach are analyzed. The region radii are considered as the important design parameters. The above two approaches are proposed for finding the region radii that optimizes the sum throughput. Monte Carlo simulations have been carried out for the verification of the optimal region radii at which the average sum throughput is maximized. The performance metrics considered are sum throughput, sub channel utilization and JI index. These metrics are analysed through simulation in Matlab 2014 version. The proposed approaches of RRP scheme is compared with the traditional SFR scheme in terms of performance metrics. The inference from the simulation result is 167.62% and 108.42% enhancement in sum throughput has achieved by heuristic and optimal region radii approach respectively. This is due to the following factors. The centre region MUEs does not caused by ICI from tier-1 macrocells. As a result, there is improvement in SNR which results increase in sum throughput. Further, the proposed RRP scheme utilized 100% of total sub channels.

3 Proposed RRP Scheme

This section presents the system model and details the heuristic and optimal region radii approach of the proposed RRP scheme.

The work flow of the proposed RRP scheme is illustrated in Fig. 1. It consists of the following modules:

- (i) Creation of LTE-A scenario
 - (ii) Region splitting based resource partitioning scheme
 - (iii) Interference analysis
 - (iv) Determination of region radii
- (a) Heuristic approach
 (b) Optimal region radii approach.

3.1 LTE-A HetNet Scenario

This section provides a detailed account of the formulation of HetNet. Figure 2 illustrates the deployment of femtocell over a macrocell in tier-1 LTE HetNet. In this scenario, the MUE is placed within the vicinity of the femtocell. Therefore, the MUE undergoes cross-tier interference as well as ICI. The cross-tier interference can occur when both the macrocell and the femtocell operate in the same sub-band. In the traditional FRF1 scheme, the MUE experiences ICI from six neighboring macrocells. Reuse factor of this kind mechanism degrades the performance of cell edge users, thereby reducing the system capacity. The proposed RRP scheme adopts FRF3 mechanism to enhance the throughput of cell edge users. This is shown in Fig. 3.

This research work has adopted the two-tier OFDMA-based cellular architecture, which consists of ‘ m ’ macrocells and ‘ f ’ femtocells, where $m = \{1, 2... K\}$ and $f = \{1, 2... L\}$, where $L=10$. Both cells are centre excited with omni directional antenna. The proposed system model consists of femtocells deployed over a macrocell formulating a HetNet. In order to analyze the impact of interference experienced by MUE, a two-tier network with seven cell structure is considered as shown in Fig. 3. The system has seven macrocells ($K=7$), out of which centre cell ‘1’ is taken as the reference cell and the remaining $K-1$

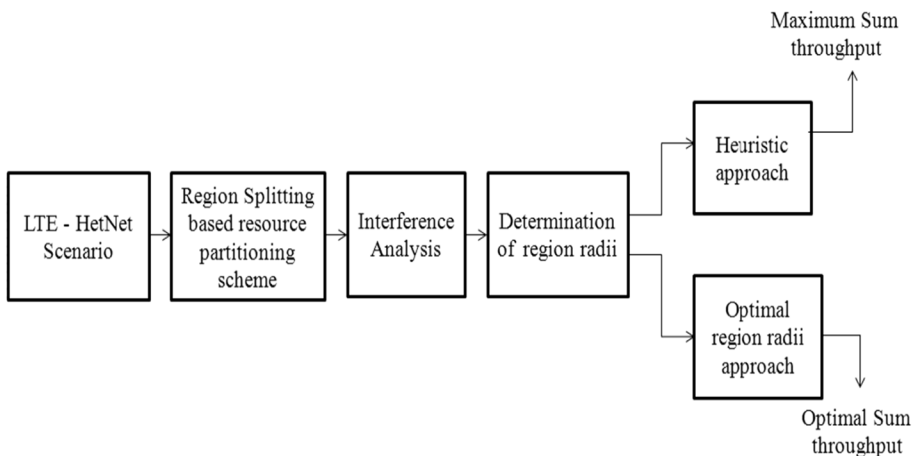


Fig. 1 Workflow of the Proposed RRP scheme

Fig. 2 LTE-A Heterogenous Network Scenario

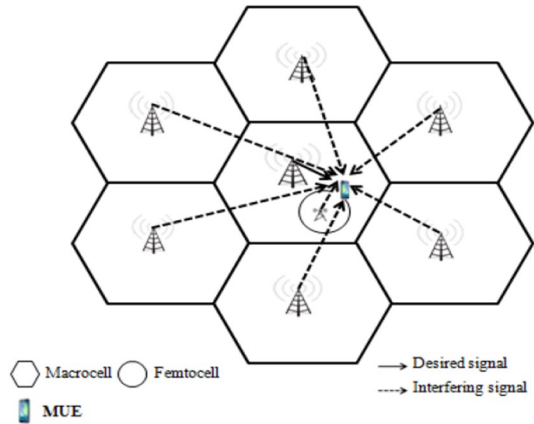
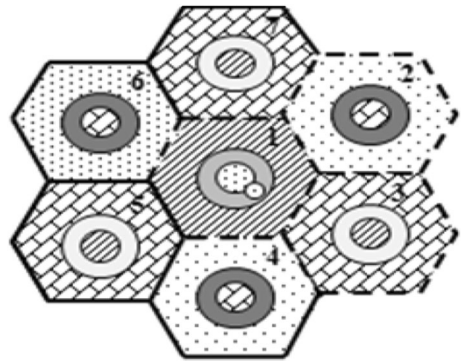


Fig. 3 Seven cell structure of two-tier network with FR3



cells are considered as interfering cells. The performance analysis is confined to the reference cell.

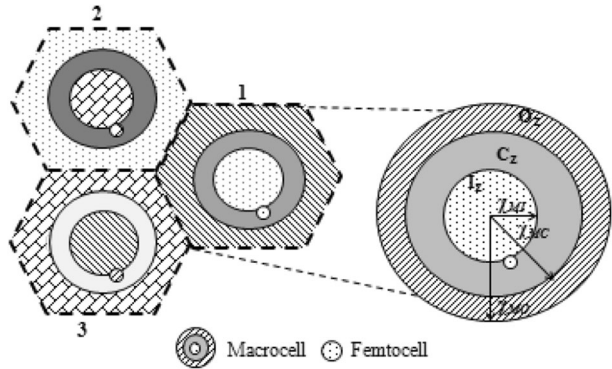
3.2 Region Splitting based Resource Partitioning

3.2.1 System Model

This section presents the system model of the proposed RRP scheme which investigates the impact of region radius on resource partitioning, sum throughput of macrocell and fairness distribution among MUEs. The system model considered Down Link (DL) transmission in the LTE HetNet scenario which is illustrated in dotted lines of Fig. 4.

Let ‘ M ’ be the macrocell which is partitioned into three regions, namely inner region (I_z), centre region (C_z), and outer region (O_z). Let χ_{MI} , χ_{MC} be the radius of I_z and C_z respectively. Similarly, χ_{MO} be the radius of the macrocell. Let $\chi_U = \{1, 2, 3, \dots, MU\}$ be the set of MUEs present in the cell, where $MU = 100$. Assume a random distribution of χ_U within the coverage of M . Hence, region radii namely inner region radius (χ_{MI}), and centre region radius (χ_{MC}) is referred as important design parameters in order to find the maximum and optimal sum throughput of macrocell. The determination of identical region radii is necessary to implement the proposed RRP scheme in the real time deployment scenario. Therefore, this research is limited to regular deployment of macrocell.

Fig. 4 System model



3.2.2 Resource Partitioning Scheme for Downlink Transmission

This section presents the resource partitioning mechanism adopted in the proposed RRP scheme for downlink transmission.

In the proposed RRP scheme, the total spectrum (β) is utilized by a cluster of three cells as shown in Fig. 4. In this strategy, β is divided into four non overlapping parts based on FRF mechanism i.e., $\beta = a \cap b \cap c \cap d$. Three parts of β are shared between I_z and O_z while the remaining one part is utilized by C_z . FRF-3 type of frequency reuse mechanism is followed during resource partitioning, which is illustrated in Fig. 5.

The total spectrum (β) is divided into four non-overlapping sub-bands, namely 'a', 'b', 'c' and 'd'. It is illustrated in Fig. 6. These sub-bands are assigned to a cluster of three cells as shown in Fig. 4. The cells 1, 2 and 3 are formed as one cluster. Further, the sub-band 'd' is partitioned into three non overlapping parts with FRF3, namely 'd₁', 'd₂', and 'd₃'. i.e., $d = d_1 \cap d_2 \cap d_3$. The sub-bands 'a', 'b', and 'c' are allocated to MUEs in outer region. Similarly, the centre region MUEs are assigned with sub-band 'd'. Here the femtocell deployed in each region, makes partial reuse of the sub-band of macrocell in order to improve the capacity of indoor users and spectral efficiency.

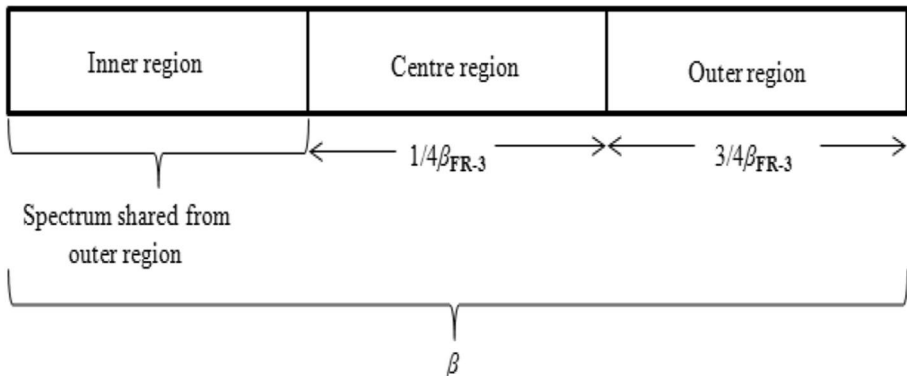


Fig. 5 Downlink spectrum allocation

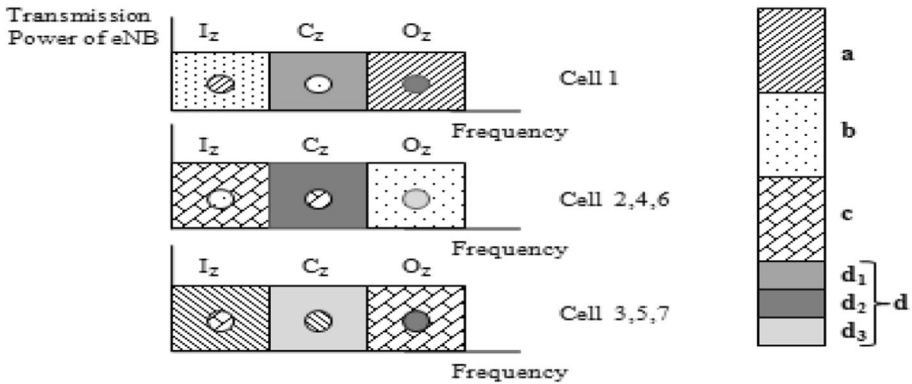


Fig. 6 Resource partitioning strategy of proposed RRP scheme

In the cluster of cells, the MUEs of O_z utilizes the sub-band of ‘a’, ‘b’ and ‘c’. This enhances the performance of cell edge MUEs by minimizing inter-cell interference. The femtocell deployed in O_z partially shares the sub-band of ‘d₂’, ‘d₃’, and ‘d₁’ that were assigned previously to the MUEs of C_z . These results in complete elimination of inter cell cross-tier interference.

Similarly, the sub-bands ‘d₁’, ‘d₂’, and ‘d₃’ are allocated to MUEs in C_z . It is to be noted that the MUEs in C_z of cell ‘1’ are not interfered by tier-1 macrocells. This results in elimination of inter-cell interference. Similarly, the femtocell deployed in the corresponding region partially shares the sub-band of ‘b’, ‘c’, and ‘a’. It is also partially shared by I_z of the same cell and O_z of neighboring cell. This reduces the inter cell cross-tier interference. For such an assignment, the intra-cell cross-tier interference would be considered closer to the transition of inner and centre region of a macrocell.

3.2.3 Allocation of Sub Channels

This section presents the calculation of sub channels for each region. The sub-bands ‘a’, ‘b’, ‘c’, and ‘d’ are formulated from 90% of β . The remaining 10% is assigned to the guard band. Let ‘ Φ ’ be the total number of available sub channels that can be assigned to both macrocell and femtocell present within the macrocell. As mentioned in the system model of the proposed RRP scheme, ‘ M ’ is divided into three regions, namely I_z , C_z , and O_z . χ_{MP} , χ_{MC} , and χ_{MO} are considered as the respective radii of the I_z , C_z , and M respectively. In a cluster of cells, the amount of sub channels required for each region is computed on the basis of their area of coverage [29].

Let ‘n’ be the cluster of cells and Φ_I, Φ_C , and Φ_O be the total sub channels required for I_z, C_z , and O_z respectively. They are computed using Eqs. (1) to (3).

Inner region:

The sub channel allocation between inner and centre region MUEs is proportional to the square of the ratio of inner region radius and centre region radius. The allocation of sub channels for inner region MUEs are given by

$$\Phi_I = \left(\frac{\pi \chi_{MI}}{\pi \chi_{MC}} \right)^2 * \Phi = \left(\frac{\chi_{MI}}{\chi_{MC}} \right)^2 * \Phi \tag{1}$$

Centre region:

The amount of sub channels required for MUEs of centre and outer region is proportional to the square of the ratio of centre region radius minus inner region radius and macrocell radius. It is calculated by using the below expression.

$$\Phi_C = \left(\frac{\pi(\chi_{MC} - \chi_{MI})}{\pi \chi_{MO}} \right)^2 * \Phi = \left(\frac{\chi_{MC} - \chi_{MI}}{\chi_{MO}} \right)^2 * \Phi \tag{2}$$

Outer region:

Similarly, the total amount of sub channels required for outer region is calculated by using Eq. (3).

$$\Phi_O = \left(\max \left[\frac{\Phi}{4}, (\Phi - (\Phi_I + \Phi_C)) \right] \right) \tag{3}$$

3.3 Interference Analysis

This section presents the analysis of performance metrics with respect to SINR experienced by MUEs in each region. The performance indices considered are sum throughput, fairness index and sub channel utilization.

The LTE-A HetNet system consists of a femtocell placed within a macrocell. According to resource partitioning strategy, the interference experienced by MUE from femtocell is taken into consideration when it is positioned within this coverage area. The investigation is restricted to the reference cell.

3.3.1 Computation of SINR

Let *IMU*, *CMU*, and *OMU* be the users deployed in the inner region, centre region, and outer region respectively. Let η_{IMU} , η_{CMU} , and η_{OMU} be the SINR experienced by the inner region, centre region, and outer region users respectively. The impact of interference is analyzed with respect to tier-1 macrocells and overlaid femtocells. The channel gain between MUE and serving eNB depends on the path loss associated with indoor user, shadowing and exponentially distributed channel fading component. For instance, when the inner region user (*IMU*) is served by eNB of macrocell ‘1’ operating in sub-band ‘b’, then the SINR experienced by *IMU* is given by [30].

$$\eta_{IMU,b} = \frac{P_{1,b} G_{1,IMU}}{N_o \Delta_f + \sum_{m=1}^{k=3} (P_{IMU,k,b} G_{IMU,k,b}) + \sum_{f=1}^L (P_{IMU,f,b} G_{IMU,f,b})} \tag{4}$$

where $P_{1,b}$ is the transmitting power. $G_{1,IMU}$ is the channel gain between *IMU* and eNB of macrocell ‘1’. N_o and Δ_f denote the noise power spectral density and the sub carrier spacing respectively. The interference experienced by *IMU* on sub-band ‘b’ is due to both ‘*K*’ adjacent cells and ‘*f*’ overlaid femtocells. It is represented in the second and third term in the denominator of Eq. (4). $P_{IMU,k,b}$ and $P_{IMU,f,b}$ are the interference power received by *IMU* from ‘*K*’ interfering macrocells of 2, 4, and 6 and nearby ‘*f*’ femtocells on sub-band

'b' respectively. $G_{IMU,k,b}$ and $G_{IMU,f,b}$ are assumed to be their corresponding channel gain. It may be noted that the interfering femtocells are considered when MUEs are within their coverage area.

Similarly, the SINR experienced by the centre region user (CMU) served by eNB of the macrocell '1' on sub-band 'd₁' is computed using Eq. (5).

$$\eta_{CMU,d_1} = \frac{P_{1,d_1} G_{1,CMU}}{N_o \Delta_f} \tag{5}$$

where P_{1,d_1} is the transmitting power of serving eNB of macrocell '1' on sub-band 'd₁'. Let $G_{1,CMU}$ be the corresponding channel gain of CMU. In this region, the interference from the neighboring 'K' adjacent cells and 'f' overlaid femtocells are completely eliminated by the resource partitioning strategy followed in the proposed scheme. Further ICI and intra cell cross-tier interference are found to be negligible.

Finally, the SINR for outer region user (OMU) is calculated using Eq. (6). It is served by eNB of macrocell '1' on sub-band 'a'

$$\eta_{OMU,a} = \frac{P_{1,a} G_{1,OMU}}{N_o \Delta_f + \sum_{m=1}^{k=3} (P_{OMU,k,a} G_{OMU,k,a})} \tag{6}$$

where $P_{1,a}$ and $G_{1,OMU}$ are their corresponding transmit power and channel gain respectively. The second term in the denominator of Eq. (6) represents the interference experienced by OMU due to 'K' interfering macrocells of 3, 5, and 7, when operated on sub-band 'a', $P_{OMU,k,a}$ and $G_{OMU,k,a}$ are the received interference power and channel gain respectively.

3.3.2 Computation of Data Rate

Let $\Psi_{MU,\chi}$ be the data rate achieved by MUEs when operated on sub-band 'χ'. It is computed using Eq. (7). Here $\chi \in \{a, b, d_1\}$ and $MU \in \{IMU, CMU, OMU\}$.

$$\Psi_{MU,\chi} = \Delta_f \log_2 (1 + \sigma \eta_{MU,\chi}) \tag{7}$$

where $\eta_{MU,\chi}$ represents the SINR experienced by MUEs in all three regions operated in various sub-band 'χ'. Here 'χ' represents 'a', 'b', & 'd₁'. Δ_f denotes the sub carrier spacing and the constant term σ denotes the target Bit Error Rate (BER) which is given by $\sigma = -1.5 / \ln(5BER)$.

3.3.3 Computation of Sum Throughput

The sum throughput (Ω_{MU}) of a serving eNB of macrocell '1' when operated on sub-band 'χ' can be expressed as below:

$$\Omega_{MU} = \sum_{MU} \sum_{\chi} \beta_{MU,\chi} \Psi_{MU,\chi} \tag{8}$$

$\beta_{MU,\chi} = 1$, represent the sub-band 'χ' assigned to MUEs, when it is not assigned, then it is zero.

3.3.4 Computation of Jain's Fairness Index

Second, Jain's Fairness Index (J_{MU}) metric is calculated to address the issue of fairness among the MUEs of the considered topology. It is expressed as the square of sum throughput of all MUEs divided by the product of the sum of squared MUEs throughput and the number of MUEs. It physically represents the deviation on throughput among MUEs. It can be calculated as follows [31]

$$J_{MU} = \frac{(\Omega_{MU})^2}{MU^* \left(\sum_{i=1}^{MU} \Psi_i^2 \right)} \quad (9)$$

The factors identified for the purpose of maximizing the sum throughput of macrocell are (i) amount of sub channels per region, (ii) number of MUEs deployed in each region, (iii) position of MUEs and (iv) region radii. The relationship between amount of sub channels and region radii are mentioned in the Eqs. 1, 2. In addition to the above factors, position and density of MUEs are also considered in the random scenario.

3.4 Determination of Region Radii

This section presents the heuristic and optimal region radii approach to determine the region radii. The performance metrics namely maximum sum throughput and optimal sum throughput are investigated from the outcome of these approaches respectively.

3.4.1 Heuristic Approach

The steps involved in the determination of region radii by heuristic approach are illustrated in Fig. 7. The proposed heuristic approach assumes a network topology which consists of macrocell, femtocell and random distribution of MUEs throughout the network topology. Then the parameters, namely the radius of macrocell (χ_{MO}) and femtocell (χ_F), number of MUEs (χ_U), and number of femtocells (L) are defined. In this approach, the radius of centre region (χ_{MC}) and its corresponding inner region radius (χ_{MI}) is varied with respect to macrocell radius (χ_{MO}). The range of χ_{MC} is varied from $0.1 \cdot \chi_{MO}$ to $0.9 \cdot \chi_{MO}$. Similarly, χ_{MI} is also varied from $0.1 \cdot \chi_{MC}$ to $0.9 \cdot \chi_{MC}$ for each fixed range of χ_{MC} . The sub channels of each region are calculated using Eqs. 1, 2, 3 for every combination of χ_{MC} and χ_{MI} . For each sub channel allocation, the proposed heuristic approach calculates the sum throughput. The above procedure is repeated for every successive inner region radius (χ_{MI}) with its corresponding fixed range of centre region radius (χ_{MC}). Thus a total contribution of 81 range of sub channel allocation is investigated. From the above investigation, the region radii which offer maximum value of sum throughput are concluded as maximum sum throughput of this approach. Hence, the corresponding region radius has been determined.

3.4.2 Optimal Region Radii Approach

Problem Formulation In the proposed heuristic approach, the following limitations are found they are (i) the resource distribution among MUEs of each region is not fairer. (ii)

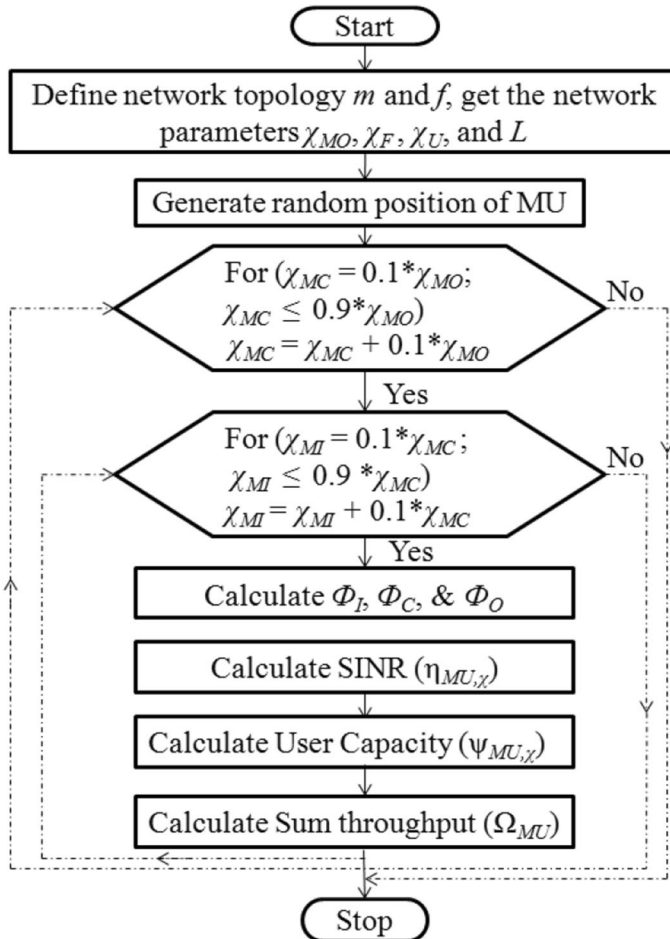


Fig. 7 Determination of region radii by heuristic approach

The minimum amount of sub channel is not allocated to certain region of macrocell. (iii) The optimal region radii are not determined. Therefore, the objective function is formulated with respect to above limitations. It is detailed below.

The objective is to maximize the sum throughput of macrocell. From the above limitations, the objective function can be formulated as follows

$$Maximize \Omega_{MU} = \sum_{i \in MU} \Psi_i^I + \Psi_i^C + \Psi_i^O \tag{10}$$

Subject to the following constraints

$$\Phi_I = \left(\frac{\chi_{MI}}{\chi_{MC}} \right)^2 * \Phi \geq \Phi_{min} \tag{11}$$

$$\Phi_C = \left(\left(\frac{\chi_{MC} - \chi_{MI}}{\chi_{MO}} \right)^2 * \Phi \right) \geq \tag{12}$$

$$\Phi_O = \max \left[\frac{\Phi}{4}, (\Phi - (\Phi_I + \Phi_C)) \right] \geq \Phi_{min} \tag{13}$$

$$I_U + C_U + O_U = \chi_U, \chi_U = \{1, 2, 3, \dots, M_U\} \tag{14}$$

$$\chi_{MI} \geq \chi_{do} \tag{15}$$

$$\Phi_{min} = 1 \ \&IMU, CMU, OMU \geq 1 \tag{16}$$

In the objective function, Eq. (10) represents the sum throughput of macrocell, where ψ^I, ψ^C , and ψ^O denote the achievable throughput of *IMU*, *CMU* and *OMU* respectively. Constraints given in Eqs. (11a) – (11c) enforce that the total number of sub channels required for each region should be greater than or equal to minimum sub channel requirement Φ_{min} . Whereas the constraint in Eq. (12) guarantees that the number of MUEs deployed in each region must be equal to the total number of MUEs per cell (MU). And constraint given in Eq. (13) insists the minimum distance between MUE and eNB. Similarly in (14), the MUEs deployed in each region must be allocated with minimum one sub channel and minimum one MUE must be positioned in each region.

An iterative based optimal region radii approach is proposed in order to find the solution of objective function. It is illustrated in Fig. 8.

In the proposed optimal region radii approach, the macrocell and random distribution of femtocell and MUEs are formulating a network topology. Then the following parameters are defined. They are radius of macrocell (χ_{MO}), radius of femtocell (χ_F), number of MUEs (χ_U), number of femtocells (L), minimum amount of sub channel (Φ_{min}), minimum distance (χ_{do}) between MUE and eNB, and total number of iterations (N) are defined. In this approach, the radius of centre region (χ_{MC}) is varied from $0.1 * \chi_{MO}$ to $0.9 * \chi_{MO}$ and its corresponding inner region radius (χ_{MI}) is varied from $0.02 * \chi_{MC}$ to $0.9 * \chi_{MC}$. With the assumption of χ_{do} and Φ_{min} , the sub channels of successive inner region radius (χ_{MI}) with its corresponding fixed range of centre region radius (χ_{MC}) are calculated using Eqs. 1, 2 3. The corresponding sum throughput is computed for each successive χ_{MI} and its corresponding χ_{MC} . The above procedure is repeated for 1000 iterations of monte carlo simulation process. Therefore, the average value of sum throughput of 1000 iterations is computed for the configured values of region radii. It is illustrated in Fig. 8. The region radii which offer maximum value of average sum throughput are concluded as optimal sum throughput. Hence, the corresponding optimal region radii have been determined.

3.5 Validation in the Proposed RRP Scheme by Optimal Region Radii Approach

The non availability of real time test bed leads to validation of the proposed RRP scheme through simulation. The randomness of MUE distribution in real time scenario is emulated using Monte Carlo simulation process by varying the iteration from 100 to 1200. The average value of sum throughput for varied iteration is computed for the configured region

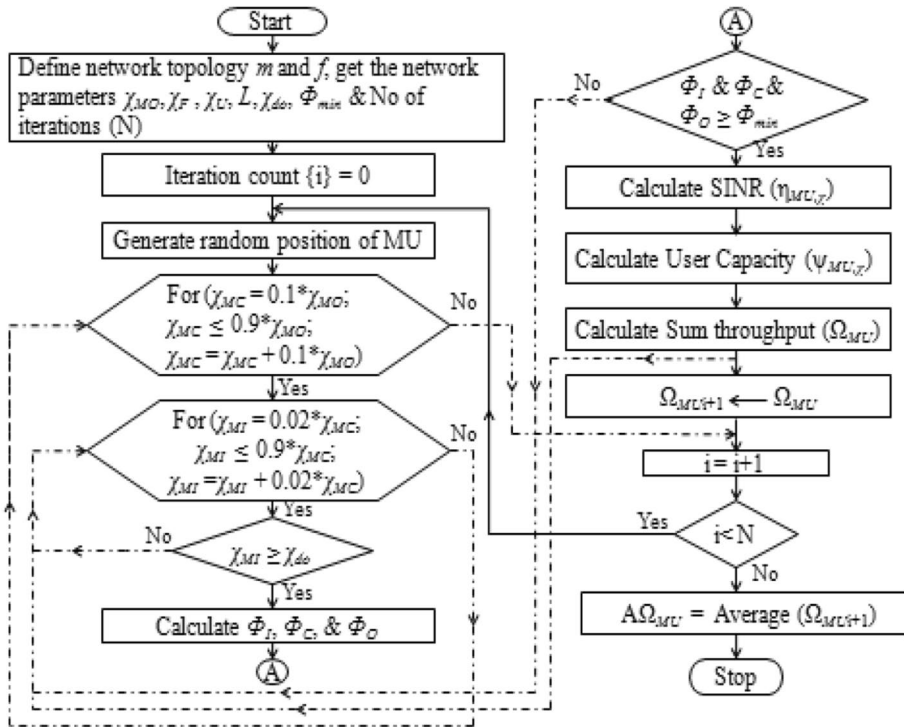


Fig. 8 Determination of region radii by optimal region radii approach

radii. The configured region radii is confined to be optimal, when the preset criteria of maximum sum throughput is met.

4 Results and Discussion

This section details the analysis of performance of the proposed RRP scheme made in terms of sum throughput, Fairness index and resource utilization by heuristic and optimal region radii approach. It is simulated by using MatLab 2014 version. In this study, maximization of sum throughput (Ω_{MU}) with respect to $\chi_{MI}, \chi_{MC}, \chi_{MO}, \Phi_I, \Phi_C,$ and Φ_O is analyzed through two approaches. Let R_I be the ratio of χ_{MI} to χ_{MC} and R_C be the ratio of χ_{MC} to χ_{MO} . In the heuristic approach, the following range of R_C and its corresponding R_I are considered. They are $R_C = \{0.1, 0.2, 0.3, \dots, 0.8, 0.9\}$ and $R_I = \{0.02, 0.04, 0.06, \dots, 0.88, 0.9\}$. Thus a total contribution of 81 ranges of region radii is investigated through the minimum assumptions.

In the optimal region radii approach, the key assumption is made in determining the optimal region radii. It is mentioned in the constraints of the objective function. With these criteria, the configured range of R_C and its corresponding R_I is obtained.

The detailed range of R_C and its corresponding R_I considered in the simulation are: (i) $R_C = 0.5; R_I = \{0.26, 0.28, 0.3, \dots, 0.48, 0.5\}$ (ii) $R_C = 0.6; R_I = \{0.26, 0.28, 0.3, \dots, 0.56, 0.58\}$ (iii) $R_C = 0.7; R_I = \{0.26, 0.28, 0.3, \dots, 0.62, 0.64\}$ (iv) $R_C = 0.8; R_I = \{0.26, 0.28,$

0.3, ...0.0.66, 0.68} and (v) $R_C = 0.9$; $R_1 = \{0.26, 0.28, 0.3, \dots 0.0.7, 0.72\}$. Thus a total contribution of 96 ranges of region radii is investigated.

The simulation parameters considered in the performance analysis are with reference to 3GPP specifications as presented in Table 1. The LTE HetNet system with 10 MHz of bandwidth comprising of 48 sub channels is considered. Each sub channel is the 180 kHz bandwidth. The indoor environment of sub urban model scenario with centre excited macrocell eNB operated in 2,000 MHz centre frequency has been considered. Further, a femtocell is randomly placed within the macrocell. Calculation of path loss is made using 3GPP propagation model [32]. Since the received power is significantly affected by shadowing and multipath fading component, it is considered as exponentially distributed with the normalized value of 1. The value of shadowing is set to be 8db.

4.1 Performance Analysis of Hueristic Approach

This section presents the impact of sum throughput of macrocell on region radii with respect to sub channel allocation and throughput contribution of each region.

Table 1 Simulation Parameters

Parameter	Value
Radius of macrocell (χ_{MO})	1000 m
Radius of femtocell (χ_F)	10 m
Carrier frequency (f_c)	2 GHz
Transmit power of eNB (P_{im})	46dBm
Transmit power femtocell (P_{if})	20dbm
System bandwidth (β)	10 MHz
Number of sub channels (Φ)	48
Minimum distance between eNB and MUE (χ_{do})	35 m
Minimum distance between indoor MUE and femtocell (χ_{Do})	<0.2 m
Propagation model: Path loss (db)between eNB and indoor MUE	$15.3 + 37.6 \log_{10} *R_1 + L_{ow}$ R ₁ in 'm'
Path loss (db) between femtocell and indoor MUE	$38.46 + 20\log_{10} *R_2 + 7db,0$ < $R_2 \leq 10$, R ₂ in 'm'
Number of eNB	1
Number of femtocell	10
Number of MUE	100
Antenna pattern	Omni directional
Modulation Scheme	64 QAM
Sub carrier spacing (Δ_f)	15 kHz
Wall penetration loss(L_{ow})	20db
White noise power density (N_o)	-174dBm/Hz

4.1.1 Impact of Sum Throughput of Macrocell on Region Radii

The impact of sum throughput of macrocell on region radii is presented in this section. In this analysis, a random distribution of MUE and femtocell within the coverage of macrocell is considered. The sum throughput of macrocell is computed by the contribution of each region. It is investigated for every fixed value of R_C and its corresponding R_I as shown in Fig. 9. From the results, it is inferred that, the sum throughput of macro cell varies from 44.37Mbps to 120.78Mbps. The maximum sum throughput of 120.78Mbps is achieved when R_C and R_I are configured to 0.9 and 0.1 respectively. From the best case, it is observed that, the percentage of sum throughput achieved in I_z, C_z , and O_z are 0%, 94.4%, and 5.57% respectively. Similarly, in the worst case, the minimum sum throughput of 44.37 Mbps is observed when $R_C = 0.8$ and $R_I = 0.7$. The corresponding contributions are 72.15%, 0% and 27.84% respectively.

In the above two cases, the following inferences are made. (i) the maximum and minimum sum throughput obtained by the major contribution made by centre region users. Therefore, it is more prominent than the other two regions. It is due to the fact that, the users of centre region of reference macrocell does not receive interference from K-1 macrocells. This resulting average SNR received by the centre region MUE is better than the inner and outer region MUE. It is illustrated in Figs. 10, 11, 12. (ii) In the best and worst case, 62.5% and 0% of total sub channels of macrocell is utilized by the centre region MUEs respectively. It is detailed in the Fig. 14. It is due to the fact that as R_C increases and its corresponding R_I decrease. Subsequently, the allocation of sub channels also increases and vice versa.

(iii) In the best case, 90% of total MUEs are positioned in the corresponding centre region coverage of macrocell such as $R_C = 0.9$. (iv) In both the cases, the contribution made by inner region MUEs are less significant due to 0% and 43.75% of total sub channels utilized by them respectively. It is shown in Fig. 13. The reason is that, the inner region MUEs are assigned with 0% sub channel allocation. And even with high percentage of sub channel utilization, its contribution is minimal due to the inter cell interference caused by tier-1 macrocells of 2, 4, and 6 respectively. This results in degradation

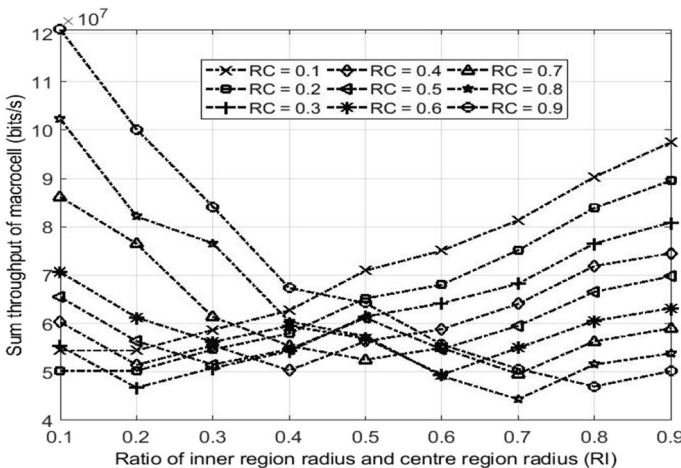


Fig. 9 Sum throughput of macrocell at R_C and R_I

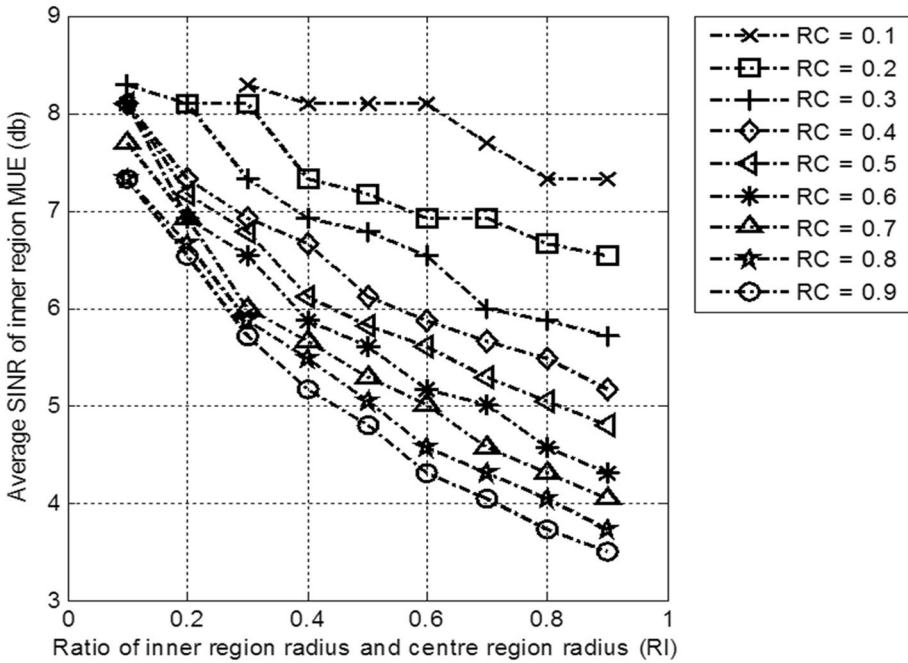


Fig. 10 Average SINR of inner region MUE

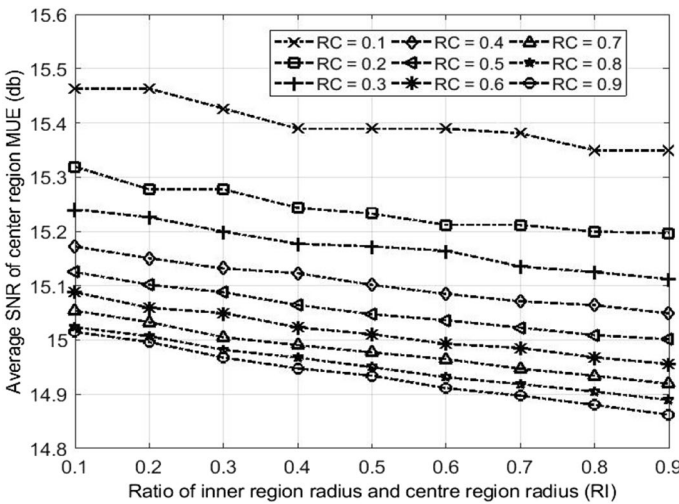


Fig. 11 Average SNR of centre region MUE

in SINR. It is illustrated in Fig. 10. (v) Similarly, in the best and worst case, 37.5% and 56.25% of total sub channels utilized by outer region MUEs respectively. It is shown in Fig. 15. The contribution made by outer region MUEs are further worsen due to severe

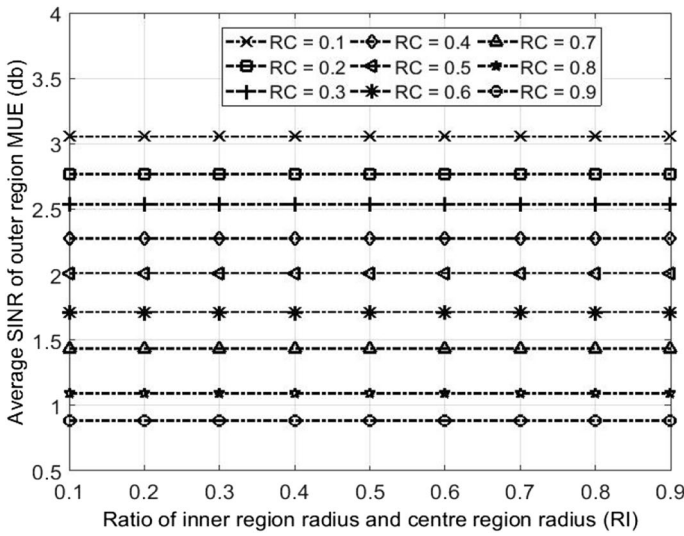


Fig. 12 Average SINR of outer region MUE

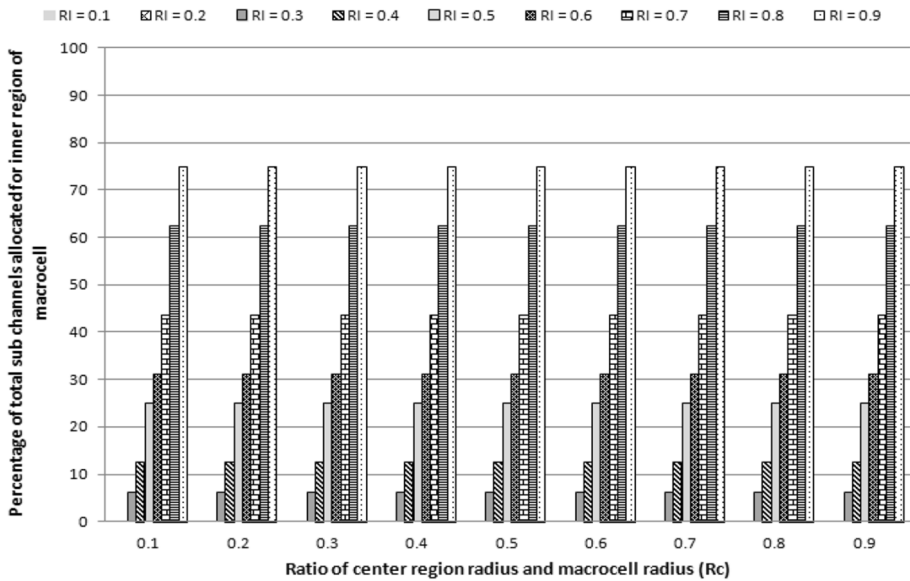


Fig. 13 Percentage of total sub channels allocated for inner region of macrocell

degradation in SINR when allocated with high percentage of sub channel. It is due to that, the ICI is caused by tier-1 macrocells of 3, 5, and 7. It is shown in Fig. 12.

From the above investigation, it is concluded that the region radii such as $R_C=0.9$ and its corresponding $R_I=0.1$ contributed maximum sum throughput. Hence, the region radii of heuristic approach have been determined.

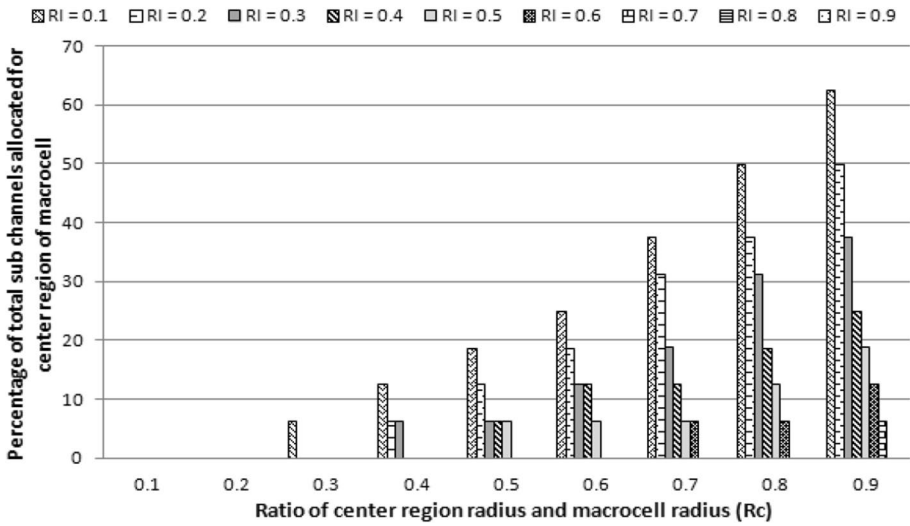


Fig. 14 Percentage of total sub channels allocated for centre region of macrocell

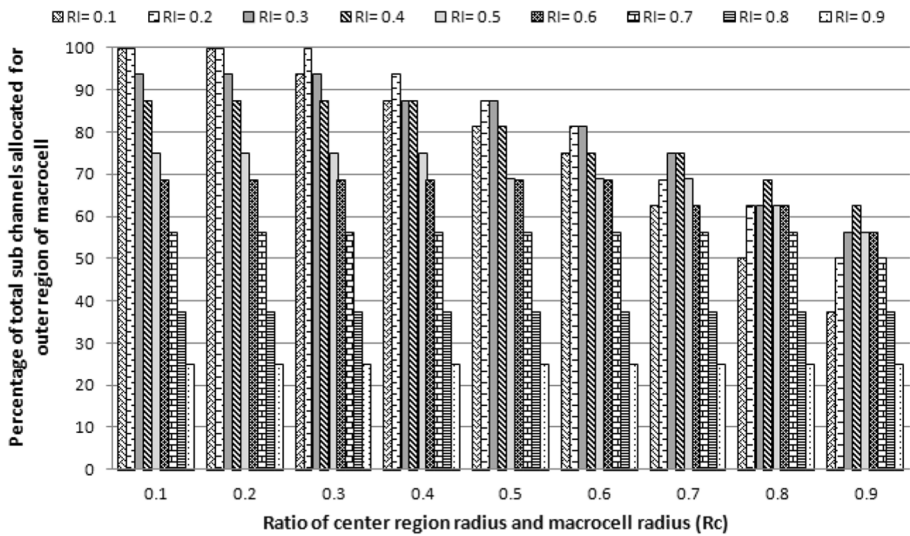


Fig. 15 Percentage of total sub channels allocated for outer region of macrocell

4.1.2 Region based SINR Analysis

This section details the average SINR experienced by MUE of each region of macrocell. Figures 10, 11 12 presents the average SINR experienced by inner, centre and outer region MUEs for fixed range of R_c and its corresponding R_1 .

Figures 10, 11 and 12 show the average SINR received by MUE of inner region, centre region and outer region respectively. It is inferred from Fig. 10 that, the average

SINR is varied from 3.49 to 8.29 db. The maximum of 8.29 db and minimum of 3.49 db is obtained at $R_C = R_I = 0.1$ and $R_C = R_I = 0.9$ respectively. The reason is that, as R_I and R_C increases, the distance of MUE from eNB also increases proportionally and vice versa. And also observed that, the inter cell interference to inner region MUE is caused by macrocells of 2, 4, and 6. It is caused by the inner region of reference macrocell 1 is sharing the same sub-band of neighbouring macrocell of outer region. In addition to ICI from tier-1 macrocells, cross tier interference from femtocell is also taken into consideration when MUE is positioned in the vicinity of femtocell.

From Fig. 11, the average SNR experienced by centre region MUE is varied from 14.86 db to 15.46 db. It is inferred that, the deviation between maximum and minimum of SNR is 0.6 db. It is due to ICI from tier-1 macrocells and intra cell cross tier interference from femtocell is completely negligible as per the proposed resource allocation strategy. This resulting the average SNR experienced by the centre region MUE is enhanced. Thereby, the sum throughput of macrocell is enhanced.

The average SINR experienced by the outer region MUE is limited to the range of 0.88 db to 3.1db. It is shown in Fig. 12. From the figure, the maximum of 3.1db and minimum of 0.88 db is observed when $R_C = 0.1$ and $R_C = 0.9$ irrespective of R_I respectively. It is obtained when R_C increases MUE distance also increases proportionally and vice versa. This results in increase in ICI from tier-1 macrocells of 3, 5 and 7. Therefore, lesser contribution on sum throughput of macrocell is obtained. And also found that, the position of MUEs would not change in the outer region by setting the fixed range of R_C .

4.1.3 Region based Sub Channel Allocation

The percentage of sub channel utilized by each region of macrocell is presented in this section. The impact of R_C and its corresponding R_I on sub channel allocation of each region is detailed.

Figures 13, 14 and 15 show the percentage of total sub channel utilized by inner, centre region and outer region MUEs respectively. It is observed from the Fig. 13 that, the minimum and maximum of 0% and 75% of total sub channels utilized by inner region MUEs when $R_I = 0.1 = 0.2$ and 0.9 respectively. It is found that as R_I increases, consequently the allocation of sub channels also increases proportionally irrespective of R_C . It is illustrated in Fig. 13.

From the Fig. 14, minimum 0% and maximum 62.5% of total sub channels utilized by the centre region MUEs of macrocell. It is inferred that, as fixed range of R_C increases such as $R_C = 0.1, 0.2, \dots, 0.9$ and its corresponding R_I decreases, subsequently, the allocation of sub channels also increases and vice versa. The maximum percentage of total sub channels allocated to this region when $R_C = 0.9$ and $R_I = 0.1$. It is shown in Fig. 14.

The maximum of 100% and minimum of 25% of total sub channels is utilized by the outer region MUEs. It is detailed in Fig. 15. It is to be noted that, as fixed range of R_C and its corresponding R_I decreases, the subsequent allocation of sub channels also increases and vice versa. The maximum and minimum percentage of total sub channel is allocated when $R_C = R_I = \{0.1, 0.2\}$ and $R_I = 0.9$ respectively.

It is concluded that, the following factors are identified for enhancing the sum throughput of macrocell. They are (i) SINR experienced by MUE of each region (ii) The sub channel allocation of each region with respect to R_C and R_I .

4.2 Performance Analysis of Optimal Region Radii Approach

4.2.1 Impact of Sum Throughput of Macrocell on Region Radii

The impact of sum throughput of macrocell on region radii is presented in this section. Using Monte Carlo simulation process, 1000 random scenario of MUE is generated. The average value of sum throughput of macrocell is computed by the total throughput of each region. It is assumed that MUEs of each region has to be allocated with minimum of one sub channel. This is the key assumption made by the optimal approach. Based on the above assumption, it is analyzed for every fixed value of R_C and its corresponding R_I as shown in Fig. 16. From the results, it is inferred that the average value of macrocell sum throughput varies from 47.367 Mbps to 94.564 Mbps. The maximum of 94.564 Mbps is achieved when R_C and R_I are configured to 0.9 and 0.26 respectively. It is considered as best case. Similarly, in the worst case of 47.367 Mbps is obtained when $R_C = 0.9$ and $R_I = 0.66$.

It is inferred that, the sum throughput contribution by MUEs of $I_2, C_2,$ and O_2 are 6.11%, 84.26% and 9.62% respectively. In the worst case, the corresponding contributions are 54.62%, 23.87% and 21.5% respectively. As mentioned earlier, the sum throughput of macrocell is enhanced by the key contribution of centre region MUEs. Therefore, the minimum of 6.25% and maximum of 43.75% of total sub channels utilized by the centre region MUEs of macrocell. It is assigned based on the key assumption.

On the other hand, the contribution made by inner region and outer region MUEs are less significant due to ICI caused by tier-1 macrocells. This is worsen the average SINR experienced by MUE of both the regions. This resulting with reduction in sum throughput of macrocell. From the investigation of 1000 iterations, the maximum value of average sum throughput is concluded as optimal sum throughput. It is obtained when $R_C = 0.9$ and $R_I = 0.26$. The corresponding region radii are referred as optimal region radii. Hence, the optimal region radii have been determined. Therefore, the macrocell with three region of proposed RRP scheme can configure the region radii as inner region radius ($\chi_{MI} = 0.26 * \chi_{MC}$, and centre region radius ($\chi_{MC} = 0.9 * \chi_{MO}$ where χ_{MO} is the macrocell radius.

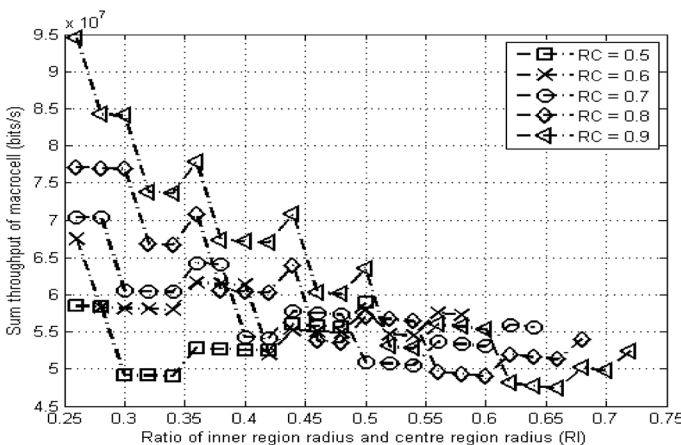


Fig. 16 Sum throughput of macrocell at R_C and its corresponding R_I

4.2.2 Optimal Sum Throughput of Macrocell for Varied Iterations of Monte Carlo Simulation

In order to validate the proposed RRP scheme in the real time environment, a wide range of distribution of MUE is emulated using Monte Carlo process. The iteration is varied from 100 to 1200. The corresponding maximum sum throughput is illustrated in Fig. 17. It is inferred that, the variation in optimal sum throughput is minimum from iteration 100 to 1200. Its value varies from 94.517 to 94.593 Mbps. Hence the service provider when operating on 10 MHz spectrum can configure the region radii as inner region radius (χ_{MI})=234 m, centre region radius (χ_{MC})=900 m, and macrocell radius (χ_{MO})=1000 m.

4.3 Comparison between Heuristic and Optimal Region Radii Approach

This section presents the comparative analysis of heuristic and optimal region radii approach. The performance is analyzed in terms of percentage of total sub channels utilized by each region, region based sum throughput and JA index. The performance of both the approaches has been analyzed under the configuration of region radii which offered maximum sum throughput and optimal sum throughput. The region radii of heuristic and optimal region radii approaches are $R_C=0.9$, $R_I=0.1$ and $R_C=0.9$, $R_I=0.26$ respectively.

4.3.1 Analysis of Region Based Resource Utilization

The percentage of sub channels utilized by each region of macrocell and total sub channel utilization of reference cell is presented in this section.

In the heuristic approach, the percentage of total sub channels allocated to I_z , C_z , and O_z are 0%, 62.5%, and 37.5% respectively. While in the optimal approach, the corresponding allocations are 6.25%, 43.75% and 50% respectively. It is inferred that, the following difference has been observed between two approaches in I_z , C_z , and O_z are 200%, 35.2%, and 28.5%. It is also observed that, the total sub channels utilized by the reference macrocell is 100% in both the approaches. It is shown in Fig. 18.

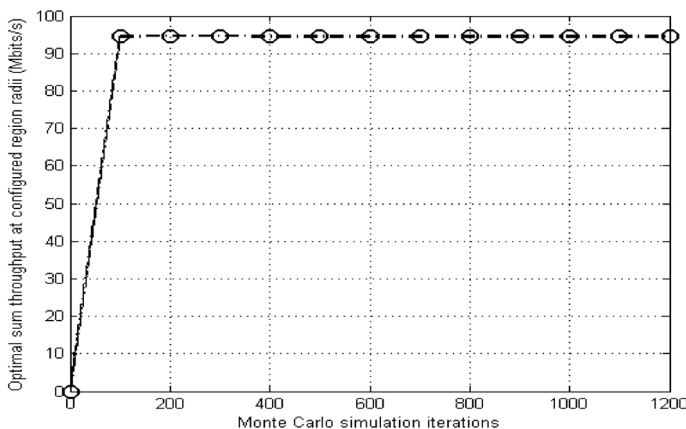


Fig. 17 Optimal Sum throughput for varied number of iterations

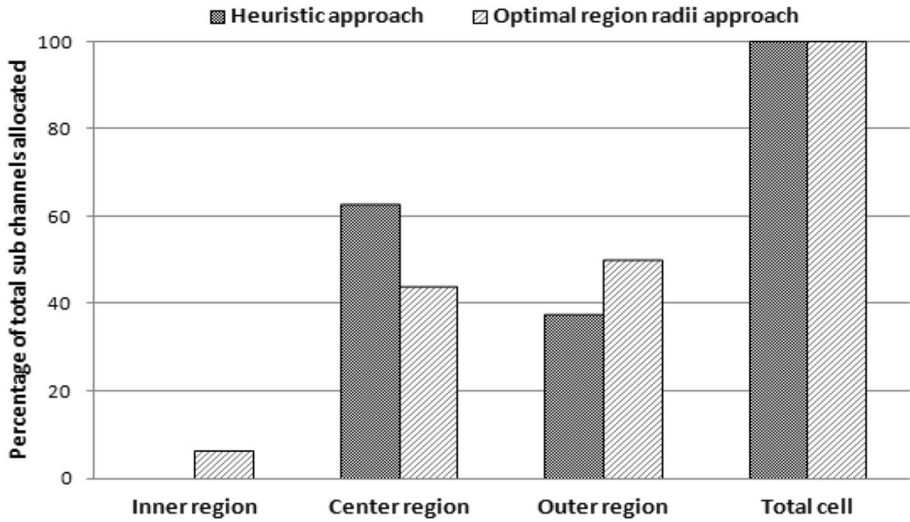


Fig. 18 Percentage of total sub channels allocated for each region of macrocell

4.3.2 Analysis of Region based Sum Throughput

This section details on the contribution of inner, centre and outer region throughput on sum throughput of macrocell by heuristic and optimal region radii approaches. It is illustrated in Fig. 19.

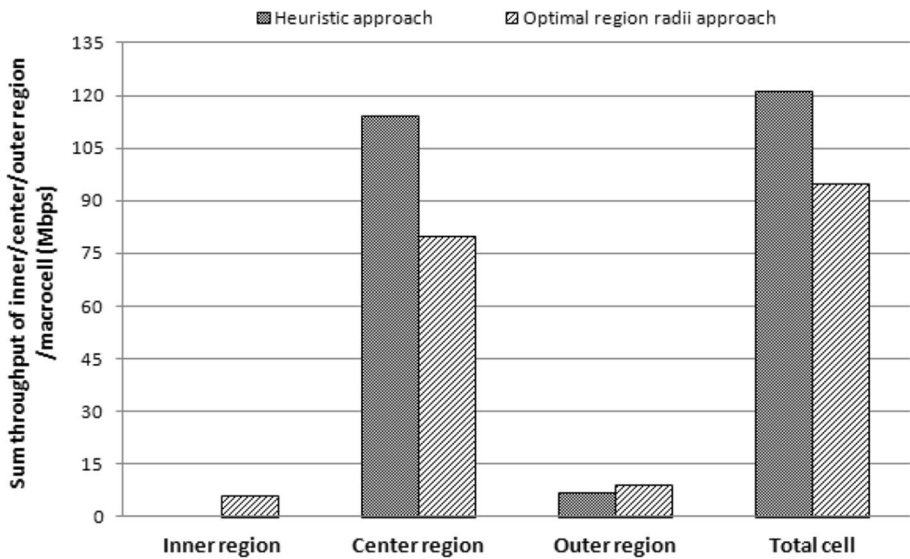


Fig. 19 Region based sum throughput of macrocell

In the heuristic approach, the sum throughput of macrocell is contributed by MUEs of $I_z, C_z,$ and O_z are 0%, 94.4%, and 5.57% respectively. Similarly in the optimal approach, the corresponding contributions are 6.11%, 84.26% and 9.62% respectively. It is inferred that, the contribution made by the centre region is more prominent. This resulting, 35.48% difference has been observed between two approaches. While in the inner and outer region, the difference is 200% and 29.8% respectively. It is due to the corresponding subchannels allocated to each region. In the heuristic approach, it is noted that, the MUEs of inner region might not receive downlink transmission if they have received very good SINR. The reason is that, 0% of sub channel allocated to the corresponding inner region radius.

4.3.3 Analysis of Jain's Fairness index

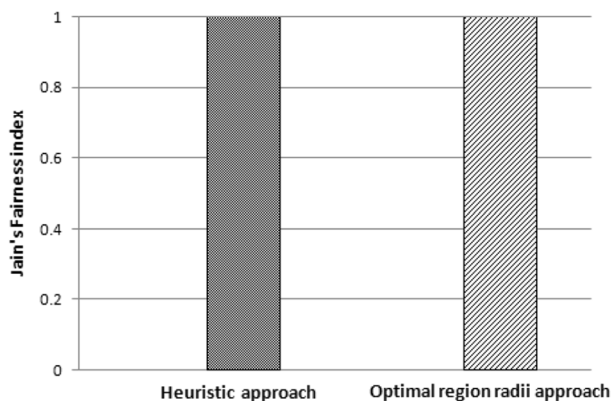
Presents the JA metric for the above two approaches. From the results, the heuristic approach attains a maximum value of 0.98. While optimal approach attains 0.95 which resulting 3.16% difference. Consequently, this difference is very minimal and concludes that the fairness among the mues is guaranteed by both the approaches.

From Fig. 20 the comparative results, the proposed RRP scheme of two approaches exhibits good results in resource utilization and JA index. On the other hand, 24.5% difference has been observed in sum throughput. Hence, the region radii is configured as $asr_c = 0.9$ and $R_I = 0.1$, when the position of MUEs are limited to greater than 9% of macrocell radius. i.e., $R_I = 0.1$. Otherwise, it is configured as $R_C = 0.9$ and $R_I = 0.26$, if MUEs are uniformly deployed over the macrocell.

4.4 Comparison of Proposed RRP Scheme by Heuristic and Optimal Region Radii Approach with SFR Scheme

This section deals with the comparison of the proposed RRP and SFR scheme by the following metrics. They are sum throughput, JA index, and utilization of total sub channels. The performance of both the schemes has been analyzed under the configuration of region radii which offered maximum sum throughput and optimal sum throughput. The region radii of heuristic and optimal region radii approach are $R_C = 0.9, R_I = 0.1$ and $R_C = 0.9, R_I = 0.26$ respectively. In addition, the optimal region radius of SFR scheme is presented in this section.

Fig. 20 Comparison of Jain's Fairness index



The performance of both schemes is analyzed with respect to the system model and simulation parameters. The system model of the FFR scheme is illustrated in Fig. 21 and that of the proposed scheme is detailed in Sect. 3. In the SFR scheme, the entire macrocell is divided into two regions, namely, centre and outer regions. In a cluster of three cells, the available bandwidth is divided into three sub-bands, namely 'a', 'b', & 'c'. It is represented in Fig. 21. These sub-bands are assigned to the outer region MUEs of macrocells '1', '2', and '3' respectively. Wherein, the MUEs of centre region are allocated with the sub-bands of outer region of neighboring macrocells [17]. The sum throughput analysis is confined to the centre cell '1' as shown in Fig. 21. The scenario considered for calculating the performance metric is random distribution of MUE and one femtocell within the macrocell. In SFR scheme, the optimal sum throughput is calculated by the simulation parameters of Table 1.

The optimal region radii which offers maximum sum throughput have been determined by the Monte Carlo simulation process of 1000 iterations. The average value of sum throughput is computed by the total throughput of each region of macrocell by 1000 iterations. It is presented in the below section.

4.4.1 Optimal Sum Throughput of SFR Scheme

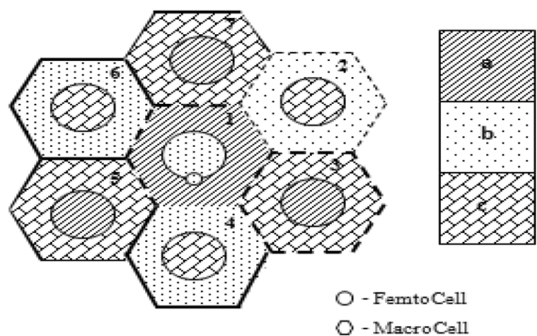
From the investigation of 1000 iterations, the average value of sum throughput is maximized at $R_C=0.9$ as shown in Fig. 22. It is obtained by the corresponding sub channels allocated to them. The percentage of total sub channels allocated to centre and outer regions are 75% and 18.75% respectively. Therefore, the region radius which offered maximum sum throughput of 45.194 Mbps is concluded as optimal sum throughput. The corresponding region radius as optimal region radius i.e., $R_C=0.9$.

4.4.2 Comparison of Region based Sum Throughput

This section presents the comparative analysis of region based sum throughput on total sum throughput by the proposed RRP and SFR scheme. It is illustrated in Fig. 23

In the proposed RRP scheme, the centre region throughput is referred as the sum throughput of inner and centre region. It is shown in Fig. 23. From the results, it is inferred that, 167.62%, and 108.42% enhancement in total sum throughput is achieved by the heuristic and optimal approach of proposed RRP scheme respectively. While in centre region, the enhancement of 172.74% and 104.43% has been obtained by heuristic and optimal

Fig. 21 System model of SFR scheme



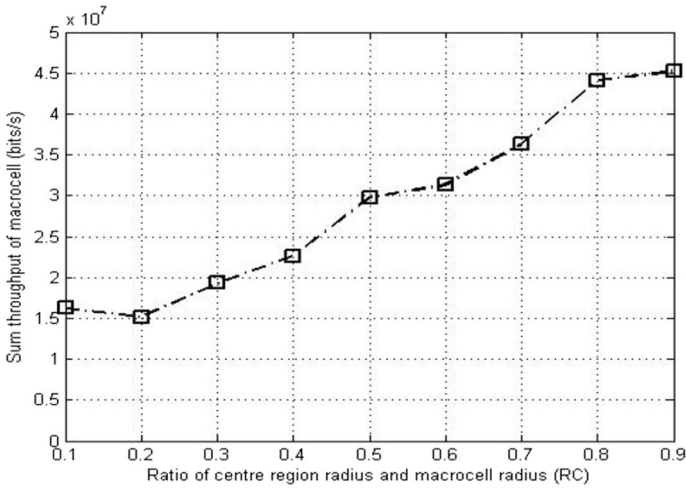


Fig. 22 Sum throughput of macrocell for varied R_C

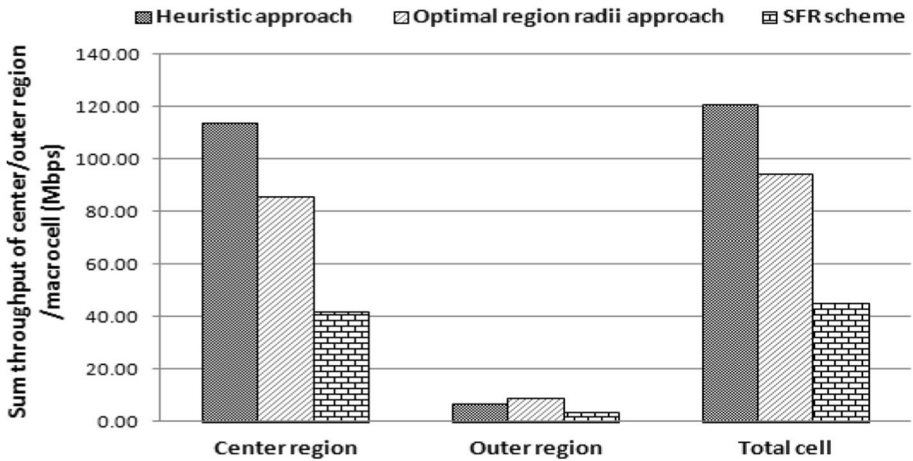


Fig. 23 Comparison of region based Sum throughput of macrocell

approach respectively. Similarly, 104.55% and 168.51% increment is achieved in outer region respectively. This is caused by the following factors. They are (i) centre region MUEs are not received ICI from the neighboring macrocells. This resulting the average SNR is enhanced. Thereby, the sum throughput of macrocell is enhanced. (ii) The total sub channels allocated to the reference macrocell is 100%.

4.4.3 Comparison of Total Sub Channel Utilization

The comparative analysis on total sub channel utilization by the proposed RRP and SFR scheme is presented in this section. It is illustrated in Fig. 24. It is inferred that, 93.75% of

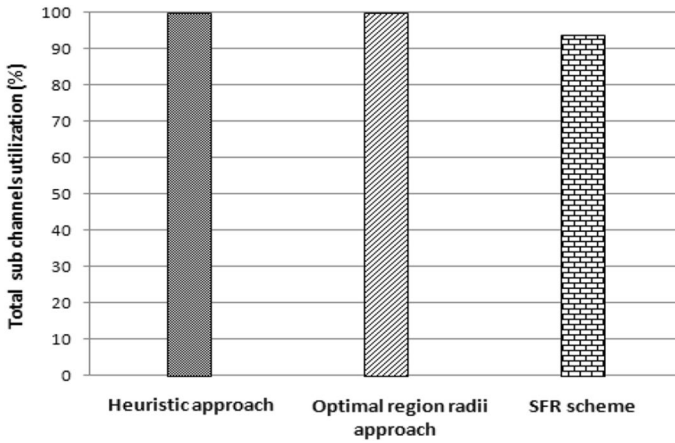


Fig. 24 Comparison of utilization of total sub channels

total sub channels utilized by the reference macrocell of SFR scheme. Wherein, 100% of total sub channels utilized by the heuristic and optimal approach of proposed RRP scheme. This shows maximum of 100% resource utilization has been accomplished. Hence, the sum throughput is further enhanced.

5 Comparative Analysis of Jain’s Fairness Index

The distribution of sub channels among the MUEs are guaranteed by the fairness index metric. The comparison of JA index of proposed RRP and SFR scheme is presented in this section. It is depicted in Fig. 25.

From the results, the maximum of 0.61 has been obtained by the SFR scheme, On the other hand, its value is 0.98 and 0.95 by the heuristic and optimal approach of proposed

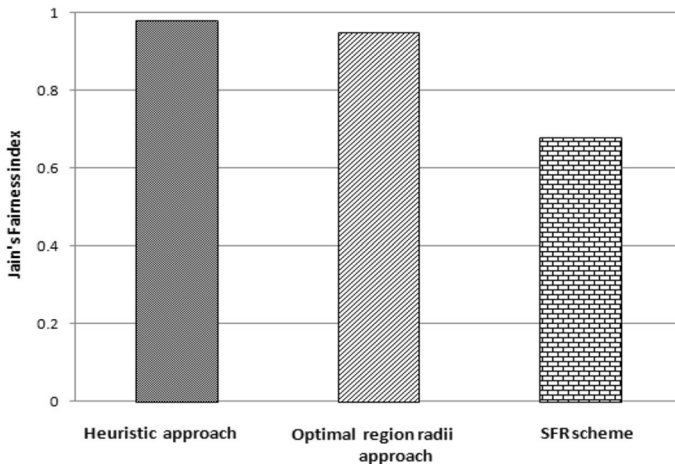


Fig. 25 Comparison of Jains Fairness index

RRP scheme. This resulting 60.6% and 55.73% enhancement is achieved by the heuristic and optimal approach respectively. Hence, the fairness among the MUEs has been guaranteed by the proposed RRP scheme.

From the above investigation, it is concluded that, the proposed RRP scheme outperforms the traditional SFR scheme by the following metrics namely, sum throughput, sub channel utilization and JA index.

6 Conclusions and Future Work

In this research work, Region splitting based Resource Partitioning Scheme (RRP) is proposed for the purpose of maximizing the sum throughput of the macrocell. In the proposed scheme, the macrocell has been partitioned into inner, centre, and outer regions. In the available system bandwidth, three parts of the spectrum have been shared by the outer region and the inner region MUEs. The remaining part has been shared by the centre region MUEs. A femtocell has been placed in each region which partially shares the sub-band of macrocell. The impact of throughput of each region contributing on sum throughput has been analyzed by the heuristic and optimal region radii approach. The radius of centre region and its corresponding inner region that maximize the sum throughput has been found by two approaches. From the result, $R_C=0.9$, $R_I=0.1$ and $R_C=0.9$, $R_I=0.26$ has been determined as the region radii that offers the maximum and optimal sum throughput of 120.95 Mbps and 94.564 Mbps respectively. Further, the real time environment for the wide range of distribution of MUE has been emulated using Monte Carlo process. The expected optimal sum throughput has been obtained for iteration ranging from 100 to 1200. The proposed RRP scheme is compared with the existing SFR scheme in terms of sum throughput, sub channel utilization and Jain's fairness index. It is inferred that 167.62% and 108.42% of enhancement in sum throughput has been achieved by the proposed RRP scheme for heuristic and optimal region radii approaches respectively.

The proposed scheme can be extended to the analysis of femtocell throughput. The static frequency reuse planning can be applied to the edge excited macro base station of LTE network to further enhance the sum throughput of macrocell. Further, the performance analysis of the proposed scheme can be extended to the irregular geometry of cellular environment.

References

1. Cisco visual networking index: Global mobile data traffic forecast update, White paper, 2017.
2. Viswanathan, H., Weldon, M., & Weldon, M. (2014). The past, present, and future of mobile communications. *Bell Labs Technical Journal*, 19(2014), 8–21.
3. 3GPP TR 25.814, V7.1.03, "Physical layer aspects for UTRA"- (Release 7), 2006.
4. Sesia, S., Toufik, I., & Baker, M. (2009). *LTE-The UMTS Long Term Evolution: From theory to Practice. Second edition*. West Sussex, U.K: Wiley.
5. Ralf Bendlin, Vikram Chandrasekhar, Runhua Chen, Anthony Ekpenyong, Eko Onggosanusi, "From homogeneous to heterogeneous networks: A 3GPP long term evolution rel. 8/9 case study", 45th IEEE Annual Conference on Information Sciences and Systems, 2011, pp. 1–5.
6. Ying, T. (2014). Jonathan and Alexey, "Recent advances in Radio resource management for heterogeneous LTE/LTE-A networks." *IEEE Communication Surveys & Tutorials*, 16(4), 2142–2180.
7. 3GPP TR 36.913 version 10.0.0, "LTE; Requirements for further advancements for Evolved Universal Terrestrial Radio Access (E-UTRA) (LTE-Advanced)"- Release 10, 2010.

8. Agiwal, M., Roy, A., & Saxena, N. (2016). Next generation 5G wireless networks: A comprehensive survey. *IEEE Communication Surveys & Tutorials*, 18(3), 1617–1655.
9. LTE to 5G Cellular and broadband innovation, White paper by Americas by Rysavy research, Aug 2017, pp. 18–44.
10. Yuan yifei and wang xinhui. (2017). “5G new Radio: Physical Layer Overview”, *International Journal on ZTE. Communications*, 15(1), 3–10.
11. Mahato, S. B., Van Do, T., Allen, B., Liu, E., & Zhang, J. (2014). Hybrid model for throughput evaluation of orthogonal frequency division multiple access networks. *IET Journal of Engineering*, 2014(3), 62–70.
12. Zhou, Yiqing, Ling Liu, Hongyan Du, Lin Tian, Xiaodong Wang, and Jinglin Shi, “An overview on inter cell interference management in mobile cellular networks: From 2G to 5G”, *IEEE International Conference on Communication Systems*, 2014, pp. 217–221.
13. Hamza, Abdelbaset S. hamza, Shady S. Khalifa, Haitham S. Hamza, and Khaled Elsayed, “A survey on inter-cell interference coordination techniques in OFDMA-based cellular networks”, *IEEE Communications Surveys & Tutorials*, Vol.15, No.4, 2013, pp.1642–1670.
14. 3GPP R1–060291, “OFDMA Downlink inter-cell interference mitigation”, Nokia 2006
15. Najjar, Abdelhalim & Hamdi, Naceur & Bouallegue, A, “Frequency Reuse Scheme with three regions in cooperative relaying for Multi-cell OFDMA Systems”, 18th telecommunications Forum (TELFOR), Serbia, Belgrade 2010, pp. 1–6.
16. Dimitrios Bilios, Christos Bouras, Vasileios Kokkinos, Andreas Papazois, Georgia Tseliou, “Selecting the Optimal Fractional Frequency Reuse Scheme in Long Term Evolution Networks”, *Springer journal on Wireless personal communication*, February 2013, pp.1–20.
17. Saquib, N. (2013). Ekram Hossain and Dong In Kim, “Fractional Frequency reuse for interference management in LTE-advanced Het Nets.” *IEEE Wireless Communications*, 20(2), 113–122.
18. Siduo and Tat M. Lok, “Dynamic Power Allocation for Downlink Interference Management in a Two-Tier OFDMA Network”, *IEEE Transactions on Vehicular Technology*, Vol. 62, No.8, October 2013, pp.4120–4125
19. Bilios, D., Bouras, C., Diles, G., Kokkinos, V., Papazois, A., Tseliou, G. (2014). A simulation framework for the evaluation of frequency reuse in LTE-A systems. *International Journal of Wireless Networks and Broadband Technologies (IJWNBT)*, 3(2), 56–83.
20. Chen, Da., Jiang, T., & Zhang, Z. (2015). Frequency partitioning methods to mitigate cross-tier interference in two-tier femtocell networks. *IEEE Transactions on Vehicular Technology*, 64(5), 1793–1805.
21. J. Zhu, N. Deng, M. Zhao and Y. Chen, “A Unified Frequency Reuse Framework for Heterogeneous Cellular Networks”, *IEEE Global Communications Conference (GLOBECOM)*, San Diego, CA, 2015, pp. 1–7.
22. Ullah, R., Faisal, N., Safdar, H., Khalid, Z., & Maqbool, W. “Fractional frequency reuse for irregular geometry based heterogeneous cellular networks”, 5th IEEE National Symposium on Information Technology: Towards New Smart World (NSITNSW), 2015, pp. 1–6
23. Mohammad T. kawser, Mohammad R. Islam, Kazi I. ahmed, Mir R. karim, Jaeed B. Saif, “Efficient Resource Allocation and Sectorization for Fractional Frequency Reuse (FFR) in LTE Femtocell Systems”, *International Journal on Radio Engineering*, Vol. 24, No. 4, December 2015, pp.940–947
24. Gajewski, S. (2017). Soft-partial frequency reuse method for LTE-A. *International Journal on Radio Engineering*, 26(1), 359–368.
25. Elwekeil, Mohamed, Masoud Alghoniemy, Osamu Muta, Adel B. Abdel Rahman, Haris Gacanin, and Hiroshi Furukawa, “Performance evaluation of an adaptive self-organizing frequency reuse approach for OFDMA downlink”, *Springer journal on wireless networks*, Aug 2017, pp.1–13
26. M. S. Hossain, F. Tariq, G. A. Safdar, N. H. Mahmood and M. R. A. Khandaker, “Multi-Layer Soft Frequency Reuse Scheme for 5G Heterogeneous Cellular Networks”, *IEEE Globecom Workshops*, Singapore, 2017, pp. 1–6
27. Xie, B., Zhang, Z., Hu, R. Q., Wu, G., & Papathanassiou, A. (Sept. 2018). Joint spectral efficiency and energy efficiency in ffr-based wireless heterogeneous networks. *IEEE Transactions on Vehicular Technology*, 67(9), 8154–8168.
28. Khan, S. A., Kavak, A., Colak, S. A., & Kucuk, K. (2019). Novel fractional frequency reuse scheme for interference management in LTE-A HetNets. *IEEE Transactions on Vehicular Technology*, 7, 109662–109672.
29. T. Novlan, Jeffrey G. Andrews, Illsoo Sohn, Radha Krishna Ganti, Arunabha Ghosh, “Comparison of Fractional Frequency Reuse Approaches in the OFDMA Cellular Downlink,” *IEEE Global telecommunication conference*, Dec 2010, pp. 1–5

30. Haipeng Lei, Lei Zhang ,Xin Zhang and Dacheng Yang “A Novel Multi-cell OFDMA System Structure using Fractional Frequency Reuse”, IEEE International symposium on Personal, Indoor and Mobile Radio Communications, Sept 2007, pp.1–5
31. Jain R., Dah Ming Chiu and W, Hawe, “A Quantitative Measure of Fairness and Discrimination for Resource Allocation in Shared Systems” Technical Report, Digital Equipment Corporation, DEC-TR-301, 1984.
32. 3GPP TS GRAN WG4 (Radio) meeting, Technical Report. R4–092042: “Simulation Assumption and parameters for FDD HeNB RF Requirements”, May 2009.

Publisher’s Note Springer Nature remains neutral with regard to jurisdictional claims in published maps and institutional affiliations.



S. Ezhilarasi received her B.E. degree of Electronics and Communication Engineering in 2000 from Madras University and M.E. in Communication Systems in 2007 from Anna University. Currently, she is pursuing Ph.D. degree in the Department of Electronics Engineering, MIT Campus, Anna University, Chennai, India. Her research area includes Communication Systems, Next Generation Wireless Networks, and Computer Networks.



P.T.V. Bhuvaneshwari received her Ph.D. degree from Anna University. She is working as Professor in the Department of Electronics Engineering, MIT Campus, Anna University. She has successfully completed five sponsored research projects. She has authored about fifty four national and international conferences and thirteen international journals. Her research focus includes Wireless Communication, Networking, IoT, and Computer Networks.